Measurement of absorbed dose to water around an electronic brachytherapy source. Comparison of two dosimetry systems: lithium formate EPR dosimeters and radiochromic EBT2 film

2015 Phys. Med. Biol. 60 3869

(http://iopscience.iop.org/0031-9155/60/9/3869)

IOP Publishing | Institute of Physics and Engineering in Medicine Physics in Medicine & Biology

Phys. Med. Biol. **60** (2015) 3869–3882 doi:10.1088/0031-9155/60/9/3869

Measurement of absorbed dose to water around an electronic brachytherapy source. Comparison of two dosimetry systems: lithium formate EPR dosimeters and radiochromic EBT2 film

Emelie Adolfsson[1,7,8], Shane White[2,7], Guillaume Landry[2,9], Eva Lund[1], Håkan Gustafsson[3], Frank Verhaegen[2,4], Brigitte Reniers[2,5], Åsa Carlsson Tedgren[1,6] and Gudrun Alm Carlsson[1]

[1] Radiation Physics, Department of Medical and Health Sciences, Linköping University, Linköping, Sweden
[2] Department of Radiation Oncology (MAASTRO), GROW—School for Oncology and Developmental Biology, Maastricht University Medical Center, Maastricht 6201 BN, the Netherlands
[3] Department of Clinical Engineering (MTÖ), Radiation Physics, Department of Medicine and Health Sciences, Linköping University, Linköping, Sweden
[4] Medical Physics Unit, Department of Oncology, McGill University, Montréal, Québec H3G 1A4, Canada
[5] Research group NuTeC, CMK, Hasselt University, Agoralaan Gebouw H, B-3590 Diepenebeek, Belgium
[6] Swedish Radiation Safety Authority, Stockholm, Sweden

E-mail: Emelie.adolfsson@regionostergotland.se

Received 2 October 2014, revised 2 January 2015
Accepted for publication 13 January 2015
Published 23 April 2015

Abstract

Interest in high dose rate (HDR) electronic brachytherapy operating at 50 kV is increasing. For quality assurance it is important to identify dosimetry systems that can measure the absorbed doses in absolute terms which is difficult in this energy region. In this work a comparison is made between two dosimetry systems, EPR lithium formate dosimeters and radiochromic EBT2 film.

[7] These authors contributed equally to this work.
[8] Author to whom any correspondence should be addressed.
[9] Currently at Ludwig-Maximilians-Universität München (LMU) Medical Physics Chair, Am Coulombwall 1, 85748 Garching, Germany

Both types of dosimeters were irradiated simultaneously in a PMMA phantom using the Axxent EBS. Absorbed dose to water was determined at distances of 10 mm, 30 mm and 50 mm from the EBS. Results were traceable to different primary standards as regards to absorbed dose to water (EPR) and air kerma (EBT2). Monte Carlo simulations were used in absolute terms as a third estimate of absorbed dose to water.

Agreement within the estimated expanded ($k = 2$) uncertainties (5% (EPR), 7% (EBT2)) was found between the results at 30 mm and 50 mm from the x-ray source. The same result was obtained in 4 repetitions of irradiation, indicating high precision in the measurements with both systems. At all distances, agreement between EPR and Monte Carlo simulations was shown as was also the case for the film measurements at 30mm and 50mm. At 10mm the geometry for the film measurements caused too large uncertainty in measured values depending on the exact position (within sub-mm distances) of the EBS and the 10 mm film results were exculded from comparison.

This work has demonstrated good performance of the lithium formate EPR dosimetry system in accordance with earlier experiments at higher photon energies (^{192}Ir HDR brachytherapy). It was also highlighted that there might be issues regarding the energy dependence and intrinsic efficiency of the EBT2 film that need to be considered for measurements using low energy sources.

Keywords: electronic brachytherapy, EPR, lithium formate, radiochromic film, intrinsic efficiency

(Some figures may appear in colour only in the online journal)

1. Introduction

Interest in using high dose rate (HDR) electronic x-ray brachytherapy sources (EBS) for accelerated partial breast irradiation (APBI) or intraoperative radiation therapy (IORT) is increasing. Due to the low tube voltage (40–50 kV) the need for radiation shielding of treatment rooms is reduced. There are also studies showing how the use of EBS for APBI results in reduced doses to normal tissues compared to ^{192}Ir HDR. However, the issue is complicated by the sensitivity of calculated doses to patient tissue composition in this energy region (Mille *et al* 2010, White *et al* 2014).

Experimental verification of dose distributions is an important feature of quality assurance in radiation therapy. It is difficult to perform dosimetric measurements around low energy (<50 keV) brachytherapy sources. Not only are dose gradients very steep, making accurate positioning and control over dose-averaging effects important, but the attenuation of photons in the keV energy region is also very sensitive to phantom material composition. It is furthermore not clear if calibrations to measure absorbed dose to water in absolute terms should be made using traceability to a primary water standard using a MV photon beam or to an air kerma standard in a kV radiation quality closer to that of the EBS. The highest accuracy in calibration coefficients in MV beams is achieved using traceability to a primary ^{60}Co water standard (Almond *et al* 1999, Andreo *et al* 2000). Calibrating absorbed dose in MV beams and measuring in kV beams, however, generally requires correcting the dosimetry system for effects of intrinsic efficiency. Intrinsic efficiency is defined as the signal per mean absorbed dose in the detector and should not be confused with the term energy dependence defined as the signal per absorbed dose to water. Various LiF thermoluminescent dosimeter (TLD)

systems have shown a response per unit absorbed dose in the detector that is about 5%–10% higher in 20–50 kV beams than in MV beams (Davis *et al* 2003, Nunn *et al* 2008, Carlsson Tedgren *et al* 2011). On the contrary, the lithium formate electron paramagnetic resonance (EPR) dosimetry system used in this work shows an approximately 6% lower response in kV than in MV beams (Adolfsson *et al* 2010). The effect of variations of intrinsic efficiency with beam quality is often neglected and has not been investigated for many dosimetry systems including EBT2 radiochromic film in photon beams. This precludes calibration in a MV beam to assure accurate dosimetry.

Our lithium formate EPR dosimetry system has been used successfully for measurements of absorbed dose to water around ^{192}Ir HDR BT sources (Antonovic *et al* 2009). The aim of this work was to test this dosimetry system for measurements of absorbed dose to water around a low energy 50 kV Axxent EBS (Xoft Inc, San Jose, CA, USA) (Rivard *et al* 2006) and to compare the results against an independent dosimetry system using radiochromic EBT2 film.

2. Materials and methods

This section is structured as follows: The theory underlying the derivation of absorbed dose to water from the measured dosimeter signal at various depths in a phantom is treated in section 2.1. Measurement techniques and calibration methods to determine absorbed dose to water are described for the EPR dosimeters in section 2.2 and for the EBT2 film in section 2.3; the geometrical set-up for the measurements with the EBS is described in section 2.4. Monte Carlo simulations to derive the energy-spectra of photons at different depths in the measurement phantom and a method to convert the results of MC calculations into absolute dose values including necessary correction factors are described in section 2.5.

2.1. Theory

2.1.1. Derivation of absorbed dose to water from the measured signal. Determination of absorbed dose to water at beam quality Q, at the distance r from the EBS, is given by

$$D_{w,Q} = D_w(r) = \frac{M_Q}{\left[\frac{M}{D_w}\right]_{Q_0}} \frac{\left[\frac{M}{D_w}\right]_{Q_0}}{\left[\frac{M}{D_w}\right]_{Q}} = \frac{M_Q}{\left[\frac{M}{D_w}\right]_{Q_0}} \frac{\left[\frac{M}{\overline{D}_{det}}\right]_{Q_0}}{\left[\frac{M}{\overline{D}_{det}}\right]_{Q}} \frac{\left[\frac{\overline{D}_{det}}{D_w}\right]_{Q_0}}{\left[\frac{\overline{D}_{det}}{D_w}\right]_{Q}} = \\ = \frac{M_Q}{\left[\frac{M}{D_w}\right]_{Q_0}} \frac{R_{Q_0}}{R_Q} \frac{\left[\frac{\overline{D}_{det}}{D_w}\right]_{Q_0}}{\left[\frac{\overline{D}_{det}}{D_w}\right]_{Q}} = \frac{M_Q}{\left[\frac{M}{D_w}\right]_{Q_0}} k_{Q,Q_0} \tag{1}$$

Here M_Q is the detector signal at beam quality Q, $[M/D_w]_{Q_0}$ is the signal per unit absorbed dose to water at the calibration beam quality Q_0, $R = M/\overline{D}_{det}$ is the signal per mean absorbed dose in the detector and is generally a function of the beam quality as indicated by the indices Q and Q_0. The quotient R_{Q_0}/R_Q corrects for different intrinsic efficiency of the detector material at calibration and at measurement. k_{Q,Q_0} is the beam quality correction factor.

Corrections were needed to convert the mean absorbed dose in the detector, $\overline{D}_{det}$ (proportional to the measured signal) to the absorbed dose, $D_{det}(r)$ in a small detector at points r, corresponding to the distances from the EBS at which the absorbed dose to water was measured. Details of the expressions used for determining the absorbed dose to water with the two detector systems and uncertainty estimations are given in the appendix A.

Table 1. Atomic composition of materials used in the MC simulations.

	Atomic composition (percentage by weight)								
Material	H	C	O	Li	N	Ar	Br	Na	Cl
Lithium formate	4.32	17.16	68.59	9.92	—	—	—	—	—
Paraffin	14.98	85.02	—	—	—	—	—	—	—
EBT2 sensitive layer lot # A090310	9.55	58.2	28.3	0.92	0.23	—	1.31	0.38	1.15
Air	—	0.012	23.18	—	75.53	1.28	—	—	—
PMMA	8.05	59.98	31.97	—	—	—	—	—	—

2.1.2. Relative intrinsic efficiency R_{Q_0}/R_Q. The intrinsic efficiency depends on the ionization densities and varies due to the linear energy transfer (LET) distribution of the secondary electrons. Intrinsic efficiency at brachytherapy beam qualities relative to ^{60}Co or MV photon beam has been thoroughly investigated for lithium formate EPR dosimeters (Adolfsson *et al* 2010). No corresponding investigations have to our knowledge been performed for radiochromic film. A complicating factor for the film is its nonlinear dose response, i.e. M/D_w and thus $M/\overline{D}_{det}$ varies not only with the LET distributions along single electron tracks but also with the magnitude of the absorbed dose in the detector with ionization densities in sensitive targets formed by overlapping electron tracks.

2.1.3. Energy absorption properties relative to water. From knowledge of M/D_w, $M/\overline{D}_{det}$ could be determined provided $D_w/\overline{D}_{det}$ is known. Values of the latter quotient have until recently been unknown for radiochromic film due to lack of knowledge of the concentrations of high atomic number materials used to increase film sensitivity (Lindsay *et al* 2010). Sutherland and Rogers (Sutherland and Rogers 2010) provided calculations of $D_w/\overline{D}_{det}$ using photon–electron transport Monte Carlo simulations and found the ratio to be close to the ratio of the mass energy absorption coefficients of the active film layer and water at photon energies <50 keV. This indicates a state of charged particle equilibrium in the active layer at these energies. It is noted that at higher photon energies this does not hold and full photon–electron transport must be simulated to obtain the mean absorbed dose in the detector.

Since May 2009, the manufacturer of EBT2 film (Ashland Inc, KY, USA) has standardized the atomic composition of the active layer (Lindsay *et al* 2010). Film lot # A090310 was used in our experiment, atomic composition of the active layer is given in table 1 (as provided by ISP, personal communication). Comparison of the ratios between the mass energy absorption coefficients for water and the active layer of three different batches of EBT2 film plus lithium formate are shown in figure 1. Mass energy absorption coefficients were taken from NIST (Hubbell and Seltzer 1995).

Figure 1 shows that the energy absorption of lithium formate relative to water varies considerably less with photon energy than the variations among the three EBT2 lots. Values of $\left[\overline{\mu}_{en}/\rho\right]^{w}_{det}$ (weighted over the energy fluences calculated for the Axxent source, see section 2.5) for lithium formate were within 0.5% at the three measurement positions, while the corresponding values for lot # A090310 were within 4%.

Results for lot # A090310 used in this work coincide with lot # 020609 as simulated by Sutherland and Rogers. It is noted that the standardized composition of the active layer results in a dosimeter with a larger energy dependence (Z_{eff} = 9.18) than lot 031109 (Z_{eff} = 7.44) at these low photon energies (Sutherland and Rogers 2010).

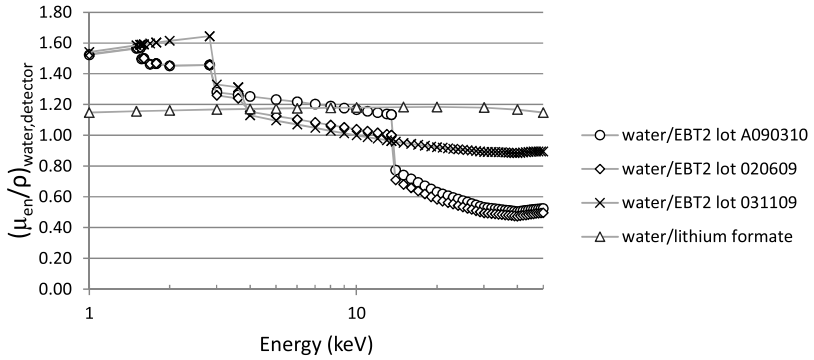

Figure 1. Mass energy absorption coefficients of water relative to lithium formate and the active layers of 3 different lots of EBT2 film; A090310 (used in this work) and 020609, 031109 investigated by Sutherland and Rogers (2010). Atomic compositions used by Sutherland and Rogers were obtained from the manufacturer.

2.1.4. Calibration methods. Calibration to measure absorbed dose to water with traceability to an absorbed dose to water primary standard presently requires the use of ^{60}Co or a MV photon beams. An alternative method with traceability to an air kerma standard was used for the film to avoid effects of the unknown intrinsic efficiency on the results of the dose measurements. Details of the calibrations of the EPR dosimeters and of the EBT2 film are given below.

2.2. Lithium formate EPR dosimeters

2.2.1. Measurement technique. The lithium formate dosimeters were cylindrical in shape with height 4.8 mm and diameter 4.5 mm. They consisted of 90% lithium formate and 10% paraffin (binding material). Signal evaluation was performed with a Bruker EleXsys E580 spectrometer, for details see earlier publications (Gustafsson *et al* 2008, Antonovic *et al* 2009, Adolfsson *et al* 2010, 2012).

2.2.2. Calibration process. Absorbed dose to water calibration was performed in a 6 MV photon beam using a Farmer type ion chamber. Due to the linear dose response of lithium formate, a two point calibration curve was used (Gustafsson *et al* 2008). The corrections necessary to convert absorbed dose to water in the calibration situation to absorbed dose to water at a specified distance from the EBS are described in the appendix A.

Two sets each of four dosimeters each were used for the calibration. One set was calibrated (in Linköping) before the EBS experiment (in Maastricht) and one set afterwards due to the time between experiment and read out of the EPR dosimeters. The results of the calibrations were the same and indicate the stability of the EPR dosimeters throughout the experiment and calibrations (Adolfsson *et al* 2012, 2014).

2.3. Radiochromic film

2.3.1. Measurement technique. The film was evaluated using a flatbed scanner Epson PRO V740 (Seiko Epson Corporation, Nagano, Japan). Image Acquisition was performed using FilmQA Pro (Version 1.0.4049.36336). All film pieces were scanned and the results were stored as TIFF images, without any colour correction, at 225dpi in words of 48 bits (16 bits per colour channel) using the RGB transmission mode for the positive film. Absorbed dose to

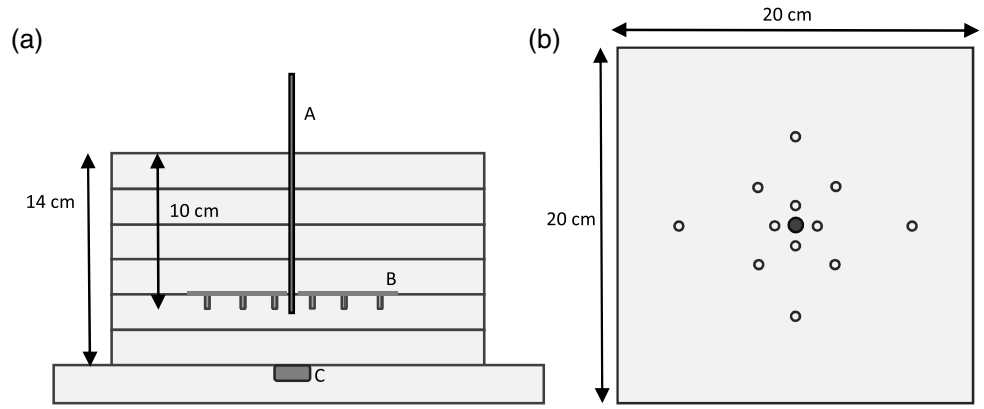

Figure 2. Schematic figure of the PMMA phantom seen from the side (*a*) and from above (*b*). Dosimeters were positioned at 10, 30 and 50 mm from the EBS (A) and the film (B) on top of the EPR dosimeters between two PMMA slabs. The Markus chamber (C) was positioned below the film dosimeter plane. Not drawn to scale. Four EPR and four EBT2 dosimeters were simultaneously irradiated at each distance.

water was derived using the triple channel method (Micke *et al* 2011, van Hoof *et al* 2012). The film was kept in light–tight folders until use and while in use, exposure to light was kept to a minimum.

2.3.2. Calibration process. The absorbed dose to water film calibration was performed using a small animal micro-irradiator with tube voltage 50 kV, 2.14 mm Al filtration and HVL = 1.54 mm Al (first layer) (PXi, North Branford, CT) (Granton *et al* 2012, van Hoof *et al* 2012). The Farmer chamber was used with traceability to a primary air kerma standard. To determine absorbed dose to water, the 'in-air method' described by the AAPM task group 61 (Ma *et al* 2001) was used with slight modifications. The micro-irradiator was to too small to use the recommended 10 × 10 cm field and the recommended 100 cm source to detector distance. Instead the field size was limited to a circular 2.5 cm diameter field and the source to detector distance was 30.7 cm (the distance to the isocentre). The calibration curve consisted of 8 dose points from 0 to 15 Gy. A full description of the micro-irradiator and the film calibration process is available elsewhere (van Hoof *et al* 2012). The corrections necessary to convert absorbed dose to water in the calibration situation to absorbed dose to water at a specified distance from the EBS are described in the appendix A.

2.4. Experimental set up for measurement in the EBS beam

A PMMA phantom previously used for EPR measurements around ^{192}Ir sources (Antonovic *et al* 2009) was used for the measurements, see figure 2. The phantom is divided into square slabs of thickness 2.5 cm stacked on one another with a centrally drilled hole (5.1 mm in diameter). The EBS fitted tightly into the hole with some compression on the sides. It was inserted to the maximum depth of the hole at each time; the positioning (as indicated by markers on the source tip) was accurate to within < 1 mm. The center of the source and the center of the EPR chips were slightly out of plane by approximately 1 mm. This was revealed in noting updated technical information about the source received after the experiment. (The updated information was taken into account when calculating the correction factors (see section 2.5)). At each distance (10, 30 and 50 mm) from the EBS, four EPR dosimeters were positioned

radially around the EBS (figure 2(*b*)). Film pieces were positioned on top of the EPR dosimeters, a circular area on the part of the film that covered the underlying EPR dosimeter cross section was marked as the region of interest. The experiment was repeated four times at 30 and 50 mm (average irradiation time was 550 s for the four repetitions). One irradiation was made at 10 mm (irradiation time 88.5 s). Due to their limited lifespan, the irradiations were performed using two EBSs. A Markus M6 ion chamber (PTW, Freiburg, Germany) situated below the dosimeter slab was used to monitor the dose delivery. The dosimeters at 30 and 50 mm were simultaneously irradiated; irradiations of dosimeters at10 mm were performed separately to avoid dose saturation of the film. The ramp-up dose of the EBS was determined to be less than 0.2% of the total administrated dose.

2.5. Monte Carlo simulations

Monte Carlo simulations were used in the derivation of corrections factors (see appendix A), to enable comparison of doses determined by EPR and film, and for calculations of the radial absorbed dose profile in the phantom. The latter dose distribution was translated into values of absorbed dose in terms of Gy using the Markus chamber (see section 2.5.3). Atomic compositions of the phantom, materials in the ERP dosimeters and the active film layer are given in table 1.

2.5.1. The Geant4 MC program. The all-purpose MC simulation toolkit Geant4 v9.3 provides a diverse set of software components that can be employed in a variety of settings, including the simulation of photon transport from low energy sources (Agostinelli *et al* 2003). In this work, the Lawrence Livermore National Laboratory low energy electromagnetic model which simulates the low energy photon interactions of the photoelectric effect, Compton scattering and Rayleigh scattering was used. The electron atomic binding effects on Compton cross sections at low energies were taken into account. The model uses the EPDL (Cullen *et al* 1997), and EADL (Perkins *et al* 1997) evaluated cross section libraries. All secondary electrons were made to deposit their energy locally due to their short range compared to typical voxel sizes; hence absorbed dose to water is approximated by water collision kerma. The cutoff energy for photons was 250 eV.

2.5.2. The geometry. A mathematical model of the PMMA phantom, EPR dosimeters and films used in the experiment was built with Geant4. The atomic compositions of the materials used are shown in table 1. The EBS source (Axxent S700) was carefully modelled in Geant4 (Agostinelli *et al* 2003) and validated by comparing measured and simulated TG-43 parameters in Rivard *et al* (2006). Using this model, 50 keV electrons were set in motion at the cathode and transported to a tungsten anode. Photons were generated via bremsstrahlung splitting (number of secondary photons equal to 100) and characteristic x-ray generation. Photons that reach the outer cooling water sheath of the source (diameter 5.1 mm) were recorded into a phase space file and then terminated. 10^9 primary electrons were simulated to generate a phase space file with 7×10^7 photons. No electrons were recorded due to their short range. The phase space source was validated against TG-43 data from Rivard *et al* (2006) to within tolerated uncertainties (<3%). This phase space source was used to simulate photon emission from the S700 in this work and has been used previously (White *et al* 2014).

Three separate simulations for each distance were run utilizing track-length scoring and two billion photon histories for each simulation. The values of photon energy fluence differential with respect to energy obtained in the simulations were used with mass-energy absorption coefficients for water to derive values of absorbed dose to water under conditions of charged particle equilibrium.

2.5.3. Converting Monte Carlo results to absolute dose values. Monte Carlo simulations were used for a third estimate of D_w in terms of Gy. Relative MC doses in terms of fGy/particle were coupled to absorbed dose to water (in Gy) at 30 mm from the EBS, determined by an independent film irradiation (unpublished results). At this irradiation, the film was positioned 30 mm from the EBS in a separate PMMA phantom with the Markus chamber perpendicularly to the beam axis. MC simulations were used to determine the relationship between the readings of the Markus chamber in the two geometries, allowing transfer of the absorbed dose to water determined in the independent film irradiation to the absorbed dose to water at 30 mm in the present experiment.

3. Results

Table 2 shows absorbed dose to water as determined by the three different systems and table 3 shows the quotients between the results of each system. In both film and EPR dosimetry systems, the absorbed dose was determined as the average of four detectors distributed around the source to minimize positional uncertainties (see figure 2). At 10 mm distance, the geometry for the film measurement caused large uncertainty in the measured values depending on the exact position (within sub-mm distances) of the EBS, therefore, the film measurement at 10 mm was left out. The EPR measurements at 10 mm were considerably less influenced by the EBS position, within 3% for an uncertainty in the EBS position of ±1 mm relative to the symmetry axis of the EPR dosimeters, the corresponding value for the film was 22%.

Agreement within the estimated expanded ($k = 2$) uncertainties (see appendix A) was found between the results obtained with the two dosimetry systems at 30 mm and 50 mm. This implies that the use of the two different calibration methodologies worked satisfactorily. The agreement between the results with the two dosimetry systems at repeated irradiations is noticeably good indicating that the type A statistical uncertainties are small for both systems. At 10 mm distance the EPR result agreed with the MC calculated value within the estimated uncertainty.

4. Discussion

4.1. Monte Carlo calculations of absorbed dose to water

The inclusion of film measurements from a separate experiment to convert the MC calculations to absorbed dose to water in absolute values (Gy) may have introduced a bias of the MC results as indicated by the good agreement between the MC calculated and film dose values at 30 mm (the depth of normalization (section 2.5.3)). The agreement between the results obtained by the EPR dosimeters and the EBT2 films in this study (tables 2 and 3) supports the validity of the adopted approach. Uncertainties in the MC calculated values are dominated by the uncertainty in the value for absorbed dose to water that was determined using film dosimetry.

4.2. Energy dependence and intrinsic efficiency of EBT2 film dosimeters

Using the results of Sutherland and Rogers 2010, it was possible to calculate the absorbed dose in the active film layer allowing analysis of the energy dependence of M/D_w published using the new standardized film in terms of $M/\overline{D}_{det}$. Brown *et al* (2012) investigated the energy response of monochromatic x-rays (25, 30 and 35 keV) with a 4 MV clinical photon beam as reference. Their results indicate variations in relative intrinsic efficiencies of $R_{25\,keV}/R_{35\,keV} = 0.95$ and $R_{25\,keV}/R_{4\,MV} = 0.63$. For a 50 kV x-ray beam (25.5 keV effective energy) relative to a 6 MV

Table 2. Results of absorbed dose to water determined by EPR dosimeters, EBT2 film and Monte Carlo simulations. The expanded (k = 2) relative uncertainties were 5% (EPR) and 7% (film) except at 10 mm where the measurement uncertainty was 6% for EPR. Uncertainty in the MC simulated doses is estimated to 7%. See table A1 in appendix for details.

	EPR D_w (Gy)			Film D_w (Gy)			MC D_w (Gy)		
Repetition	10 mm	30 mm	50 mm	10 mm	30 mm	50 mm	10 mm	30 mm	50 mm
1	9.4	10.7	2.6	—	10.1	2.6	9.4	10.3	2.4
2		10.5	2.5		10.0	2.6		10.2	2.4
3		10.8	2.6		10.3	2.7		10.5	2.5
4		9.6	2.3		9.1	2.4		9.3	2.2

Table 3. The quotient of results displayed in table 2.

	D_w(EPR)/D_w(MC)			D_w(film)/D_w(MC)			D_w(EPR)/D_w(film)		
Repetition	10 mm	30 mm	50 mm	10 mm	30 mm	50 mm	10 mm	30 mm	50 mm
1	1.01	1.04	1.08	—	0.98	1.08	—	1.05	0.99
2		1.03	1.05		0.98	1.09		1.05	0.96
3		1.03	1.07		0.97	1.09		1.05	0.98
4		1.03	1.05		0.98	1.08		1.05	0.97

photon beam (effective energy 1.4 MeV) results by Butson *et al* (2010) indicate a relative intrinsic efficiency of $R_{50\,kV}/R_{1.4\,MeV} = 0.57$, consistent with the result $R_{25\,keV}/R_{4\,MV} = 0.63$ of Brown *et al*. Arjomandy *et al* (2012) measured depth doses in water at 75 kV. Dose response calibration was performed at 75 kV. Compared to measurements with an ion chamber, the film showed an over-response of 8–9% at a depth of 10 cm compared to the normalization depth of 2 cm. The effective energy was noted to increase from 32.1 keV to 38.4 keV. Only 3% of this increase can be assigned to an increase in the energy absorption of the film relative to water indicating an increase in relative intrinsic efficiency consistent with the results of Brown *et al*. An increase in effective energy of only 1 keV, from 34 keV to 35 keV in our EBS measurements at 50 mm compared to 30 mm is not likely to have a noticeable effect on the results. It may be of some interest here to note that Kirby *et al* (2010) noted an under-response of 0.6 for the EBT2 film in the Bragg-peak of protons and suggested a model of explanation similar to those used in explaining the relative intrinsic efficiency of low energy photons relative to MV photon beams for TLDs and EPR dosimeters.

4.3. Comparison of two methods of calibration

Calibration of the EPR dosimeters to measure absorbed dose to water was made using a 6 MV linear accelerator. Correction factors to allow use of the calibrated dosimeters at low photon energies (<50 keV) included a correction for the decrease in intrinsic efficiency of the dosimeters at the beam quality used at measurements compared to that used at calibration (Adolfsson *et al* 2010). This is an important correction commonly not considered in the literature. The uncertainties added due to these corrections were not very large as can be seen in the uncertainty budget (table A1, sources 3–6). Since the variation in intrinsic efficiency with beam quality of the EBT2 film is not known use of a suitable x-ray source was the only option for accurate dosimetry with the radiochromic film dosimetry system. The uncertainty budget shows that the combined standard uncertainty was somewhat lower using the EPR dosimetry

and its MV based calibration system. Transfer of the air kerma calibration coefficient from the primary lab to the experimental lab at low tube voltages is associated with larger uncertainty than the corresponding transfer of the calibration coefficient from a primary ^{60}Co water standard to the higher energy MV beams and, in addition, there is an uncertainty associated with transforming air kerma to water kerma. The energy absorption properties of the detector relative to water also influence measurement uncertainty. The energy absorption properties of lithium formate are considerably closer to water than those of the EBT2 film (see figure 1) which depends on small, less known concentrations of high atomic number materials in the film active layer. The change in the ratio of mass energy absorption coefficients between water and the active layer of the EBT2 film is as large as 4% from the 10 mm to the 50 mm depth whereas the corresponding value for the EPR dosimeters is only 0.5%.

5. Conclusions

This work is a contribution to developing reliable experimental methods suitable for dosimetry around low energy brachytherapy sources, in particular high dose rate EBS. The EPR dosimeters were found to yield results in agreement with Monte Carlo simulations at three distances (10, 30 and 50 mm) from the source in the phantom. The EBT2 films agreed with Monte Carlo and EPR at 30 mm and 50 mm. At 10 mm, the uncertainty in the exact positioning of the EBS was too large to get a reliable estimate using EBT2 films. This work has shown the complexity of measurements around this type of source and the importance of detailed knowledge of the properties of the dosimetry system used. It was also shown that lithium formate EPR dosimetry is a good candidate for the purpose and it was deduced that there might be issues regarding energy dependence and intrinsic efficiency of the EBT2 film that need to be considered in future measurements.

Acknowledgments

This work was supported by the Swedish Cancer Foundation Grants CAN 2012/764 and CAN 2009/1113 and by Grant #2011–700810 of the Canadian Cancer Society Research Institute (CCSRI). SW was funded by MAASTRO-Atrium research grant. GL was supported by the Natural Sciences and Engineering Research Council of Canada (NSERC) and by the O'Brien Foundation. BR was supported by a Marie Curie Reintegration Grant (Grant Agreement No. PIRG05-GA-2009-247878 from FP7-PEOPLE-2009-RG). HG acknowledges The Swedish Research Council (diarienr 2009-5430). Xoft, Inc and Ashland Inc., KY, USA are gratefully acknowledged for providing technical details for the simulations and experiments.

Appendix A

A.1. Determination of absorbed dose to water with EPR dosimeters

Determination of absorbed dose to water using EPR dosimeters in the PMMA phantom at a distance r from the source follows equation (A.1).

$$D_{\mathrm{w,phan,50\,kV}}(r) = M_{\mathrm{50\,kV}}\left(r\right)\left[\frac{D_{\mathrm{w}}}{M}\left[{}_{\mathrm{m}}\,\overline{s}_{\mathrm{col}}\right]_{\mathrm{w}}^{\mathrm{PMMA}}\overline{f}_{\mathrm{B}}\right]_{\mathrm{6\,MV}}\frac{R_{\mathrm{Q_0}}}{R_{\mathrm{Q}}}\left[\frac{\overline{\mu}_{\mathrm{en}}}{\rho}\right]_{\mathrm{det}}^{\mathrm{w}}f_{\mathrm{vol}}\frac{\overline{D}_{\mathrm{det,MC}}}{\overline{D}_{\mathrm{lithium\ formate}}} \tag{A.1}$$

Table A1. Components contributing to the combined relative standard uncertainty for EPR dosimeters and EBT2 film.

	Distance (mm)				Distance (mm)	
Source of uncertainty EPR	10	30	50	Source of uncertainty EBT2	30	50
1. $u(M_{50\,\mathrm{kV}})/M_{50\,\mathrm{kV}}$	0.4%	0.4%	0.4%	1. $u(M)/M$	0.5%	0.5%
2. $u(D_w/M)/D_w/M$	1.7%	1.7%	1.7%	2. $u(M/K_{air})/M/K_{air}$	2.1%	2.1%
3. $u({}_m\bar{s}_{col})_w^{PMMA}/({}_m\bar{s}_{col})_w^{PMMA}$	0.5%	0.5%	0.5%	3. $u\left(\left[\frac{\bar{\mu}_{en}}{\rho}\right]_w^{air}\right)/\left[\frac{\bar{\mu}_{en}}{\rho}\right]_w^{air}$	1.5%	1.5%
4. $u(\bar{f}_B)/\bar{f}_B$	0.5%	0.5%	0.5%	4. $\frac{u\left(\left[\frac{\bar{\mu}_{en}}{\rho}\right]_{w,phan}^{det}\left[\frac{\bar{\mu}_{en}}{\rho}\right]_{det,cal}^{w}\right)}{\left[\frac{\bar{\mu}_{en}}{\rho}\right]_{w,phan}^{det}\left[\frac{\bar{\mu}_{en}}{\rho}\right]_{det,cal}^{w}}$	1.5%	2.0%
5. $u(R_{Q_0}/R_Q)/\left(R_{Q_0}/R_Q\right)$	1.0%	1.0%	1.0%	5. $u(R_{Q_0}/R_Q)/\left(R_{Q_0}/R_Q\right)$	—	—
6. $u\left(\left[\frac{\bar{\mu}_{en}}{\rho}\right]_{det}^{w}\right)/\left[\frac{\bar{\mu}_{en}}{\rho}\right]_{det}^{w}$	0.5%	0.5%	0.5%	6. $u(f_{pos})/f_{pos}$	1.0%	1.0%
7. $u(f_{pos})/f_{pos}$	1.5%	0.5%	0.5%	7. $u(f_{vol})/f_{vol}$	1.0%	1.0%
8. $u(f_{vol})/f_{vol}$	1.0%	1.0%	1.0%			
9. $u\left(\frac{\bar{D}_{det,MC}}{\bar{D}_{lithium\ formate}}\right)/\frac{\bar{D}_{det,MC}}{\bar{D}_{lithium\ formate}}$	0.5%	0.5%	0.5%			
Combined 1–9				**Combined 1–7**		
$u(D_{w,phan,50\,kV}(r))/D_{w,phan,50\,kV}(r)$	3%	2.5%	2.5%	$u(D_{w,phan,50\,kV}(r))/D_{w,phan,50\,kV}(r)$	3.3 %	3.6%

where M denotes the EPR signal, $[{}_{\mathrm{m}}\bar{s}_{\mathrm{col}}]_{\mathrm{w}}^{\mathrm{PMMA}}$ is the mass collision stopping power ratio between PMMA and water and converts absorbed dose to water to absorbed dose to PMMA; $\overline{f}_{\mathrm{B}} = \overline{D}_{\mathrm{det}}/D_{\mathrm{PMMA}}$ is the Burlin cavity theory coefficient and converts absorbed dose to PMMA to the mean absorbed dose in the detector (film active layer). Detailed information and numerical values of these factors are found in Antonovic *et al* (2009). $R_{\mathrm{Q_0}}/R_{\mathrm{Q}}$ is the correction for intrinsic efficiency (Adolfsson *et al* 2010) and was set to 1.06.

The values of $\left[\overline{\mu}_{\mathrm{en}}/\rho\right]_{\mathrm{det}}^{\mathrm{w}}$ were determined to be 1.249, 1.246 and 1.243 at 10 mm, 30 mm and 50 mm respectively by weighting over the photon energy fluence spectrum at the three measurement positions in the phantom. Mass energy absorption coefficients were taken from NIST (Hubbell and Seltzer 1995). The volume averaging correction factor, f_{vol}, was calculated with MC as the quotient of the absorbed dose to a 1 mm^3 'point detector' situated at the centre of the EPR dosimeter and the absorbed dose to the full size detector. The values of f_{vol} at 10, 30 and 50 mm were 1.020, 1.023, and 1.030 respectively. The last factor in equation (A.1) is needed to account for the fact that the signal is proportional to the dose registered in the lithium formate grains and not to that registered in the surrounding paraffin. This factor was calculated using MC simulations as described in detail by Adolfsson *et al* (2010).

A.2. Determination of absorbed dose to water with EBT2 film

Determination of absorbed dose to water using the EBT2 film in the PMMA phantom at the distance r from the source followed equation (A.2)

$$D_{\mathrm{w,phan,50kV}}(r) = \frac{M_{\mathrm{phan}(r)}\left[\frac{M}{D_{\mathrm{w}}}\right]_{\mathrm{cal,50\,kV}}}{\left[\frac{M}{D_{\mathrm{w}}}\right]_{\mathrm{cal,50\,kV}}\left[\frac{M}{D_{\mathrm{w}}}\right]_{\mathrm{phan},r}} f_{\mathrm{pos}} f_{\mathrm{vol}} = \frac{M_{\mathrm{phan}(r)}\left[\frac{\overline{\mu}_{\mathrm{en}}}{\rho}\right]_{\mathrm{w,cal,50\,kV}}^{\mathrm{det}}}{\left[\frac{M}{D_{\mathrm{w}}}\right]_{\mathrm{cal,50\,kV}}\left[\frac{\overline{\mu}_{\mathrm{en}}}{\rho}\right]_{\mathrm{w,phan},r}^{\mathrm{det}}} \frac{R_{\mathrm{Q_0}}}{R_{\mathrm{Q}}} f_{\mathrm{pos}} f_{\mathrm{vol}} \qquad \text{(A.2)}$$

The film was calibrated to measure air kerma free-in-air using the TG61 protocol (Ma *et al* 2001). Absorbed dose to water was calculated by multiplying air kerma with the ratio of the weighted mean of the mass energy absorption coefficients for water and air yielding water kerma, i.e. absorbed dose to water under charged particle equilibrium. The quotient $\left[\overline{\mu}_{\mathrm{en}}/\rho\right]_{\mathrm{w,cal,50\,kV}}^{\mathrm{det}}/\left[\overline{\mu}_{\mathrm{en}}/\rho\right]_{\mathrm{w,phan},r}^{\mathrm{det}}$ was set to unity. A correction for film position in the phantom f_{pos} was derived by MC calculation of the absorbed dose to water in the volume occupied by the film in the experiment and the same volume positioned at the centre of the EPR dosimeters (in the absence of the EPR dosimeter). Numerical values at 30 and 50 mm were 1.020 and 1.030 respectively. A volume averaging factor f_{vol} for the film was applied, derived similarly to the volume averaging for the EPR dosimeters. The quotient of the absorbed dose to a 'film point' (1 mm^3) and the absorbed dose to the full size film area was calculated. Numerical values at 30 and 50 mm were 0.991 and 0.976 respectively.

In the last equality of equation (A.2) it is assumed that the signal from the film is proportional to the mean absorbed dose to the detector. The factor $R_{\mathrm{Q_0}}/R_{\mathrm{Q}}$ takes into account any deviation from this assumption caused by different LET distributions of the secondary electrons at calibration and in the measurement in the PMMA phantom. Here, $R_{\mathrm{Q_0}}/R_{\mathrm{Q}}$ was assumed to be unity.

A.3. Uncertainty in the experimentally determined absorbed dose

The total combined relative standard uncertainties in absorbed dose $u(D_{w,phan,50\,kV}(r))$ / $D_{w,phan,50kV}(r)$, derived from equations (A.1) and (A.2) were estimated by quadratically adding the relative standard uncertainties of its parameters (JCGM 2008)). Derivation of the uncertainties for the EPR dosimeters was described in detail in (Antonovic *et al* 2009, Adolfsson *et al* 2010). The estimated uncertainties are presented in table A1.

Estimates of the relative standard uncertainties related to the film calibration (points 2 and 3 in table A1) were taken from the AAPM protocol (Ma *et al* 2001). The mass-energy absorption correction factor (point 4 in table A1) was set to unity. However, for a film with the composition of the active layer in table 1 (the film used in this work), corrections of 0.975 and 0.966 at 30 mm and 50 mm, respectively, should be applied. This correction was not introduced in calculating $D_{w,phan,50\,kV}(r)$ since it cannot be ascertained that the atomic composition is exactly that aimed at by the manufacturer. Instead, we used the information in figure 1 to estimate uncertainties caused by neglecting the correction. Assuming maximum possible deviations of 2.5% (30 mm) and 3.4% (50 mm) from unity for this factor, standard uncertainties were obtained by dividing with $\sqrt{3}$ (assuming a triangular probability distribution).

The uncertainty in MC calculated doses depend on the statistical uncertainty in the MC simulations, the uncertainty in the film dose at the normalization depth (30 mm) and a correction to account for the different positions of the Markus chamber in the experiment used for normalization (perpendicular to the beam axis) and in the experiment itself (see figure 2). The combined relative standard uncertainty was estimated to be 3.5%.

References

Adolfsson E, Carlsson Tedgren Å, Alm Carlsson G, Gustafsson H and Lund E 2014 Optimisation of an EPR dosimetry system for robust and high precision dosimetry *Radiat. Meas.* **70** 21–8

Adolfsson E *et al* 2010 Response of lithium formate EPR dosimeters at photon energies relevant to the dosimetry of brachytherapy *Med. Phys.* **37** 4946–59

Adolfsson E *et al* 2012 Investigation of signal fading in lithium formate EPR dosimeters using a new sensitive method *Phys. Med. Biol.* **57** 2209–17

Agostinelli S *et al* 2003 GEANT4—a simulation toolkit *Nucl. Instrum. Methods Phys. Res.* **506** 250–303

Almond P *et al* 1999 AAPM's TG-51 protocol for clinical reference dosimetry of high-energy photon and electron beams *Med. Phys.* **26** 1847–70

Andreo P *et al* 2000 *Absorbed Dose Determination in External Beam Radiotherapy, IAEA TRS 398: an International Code of Practice for Dosimetry Based on Standards of Absorbed Dose to Water (IAEA Technical Report Series vol 398)* (Vienna: International Atomic Energy Agency)

Antonovic L, Gustafsson H, Alm Carlsson G and Carlsson Tedgren Å 2009 Evaluation of a lithium formate EPR dosimetry system for dose measurements around ^{192}Ir brachytherapy sources *Med. Phys.* **36** 2236–47

Arjomandy B, Tailor R, Zhao L and Devic S 2012 EBT2 film as a depth-dose measurement tool for radiotherapy beams over a wide range of energies and modalities *Med. Phys.* **39** 912–21

Brown T A D *et al* 2012 Dose-response curve of EBT, EBT2, and EBT3 radiochromic films to synchrotron-produced monochromatic x-ray beams *Med. Phys.* **39** 7412–7

Butson M J, Yu P K N, Cheung T and Alnawaf H 2010 Energy response of the new EBT2 Radiochromic film to x-ray radiation *Radiat. Meas.* **45** 836–9

Carlsson Tedgren Å, Hedman A, Grindborg J-E and Carlsson G A 2011 Response of LiF:Mg,Ti thermoluminescent dosimeters at photon energies relevant to the dosimetry of brachytherapy (<1 MeV) *Med. Phys.* **38** 5539–50

Cullen D, Hubbell J H and Kissel L 1997 EPDL97: the evaluated photon data library 97 version UCRL-50400 **6**

Davis S D *et al* 2003 The response of LiF thermoluminescence dosimeters to photon beams in the energy range from 30 kV x-rays to ^{60}Co gamma rays *Radiat. Prot. Dosim.* **106** 33–43

Granton P V *et al* 2012 A combined dose calculation and verification method for a small animal precision irradiator based on onboard imaging *Med. Phys.* **39** 4155–66

Gustafsson H, Lund E and Olsson S 2008 Lithium formate EPR dosimetry for verification of calculated dose distributions prior to intensity modulated radiation therapy *Phys. Med. Biol.* **53** 4667–82

Hubbell J H and Seltzer S M 1995 *Tables of X-ray Mass Attenuation Coefficients and Mass Energy-Absorption Coefficients 1 keV to 20 for Elements Z = 1–92 and 48 Additional Substances of Dosimetric Interest* (Washington, DC: NIST)

JCGM 2008 Evaluation of measurement data *Guide to the Expression of Uncertainty in Measurement (No. JCGM 100:2008) (Joint Committee for Guides in Metrology)* (Boulder, CO: NCSL International)

Kirby D *et al* 2010 LET dependence of GafChromic films and ion chamber in low-energy proton dosimetry *Phys. Med. Biol.* **55** 417–33

Lindsay P, Rink A, Ruschin M and Jaffray D 2010 Investigation of energy dependence of EBT and EBT-2 Gafchromic film *Med. Phys.* **37** 571–6

Ma C-M *et al* 2001 AAPM protocol for 40–300 kV x-ray beam dosimetry in radiotherapy and radiobiology *Med. Phys.* **28** 868–93

Micke A, Lewis D F and Yu X 2011 Multichannel film dosimetry with nonuniformity correction *Med. Phys.* **38** 2523–34

Mille M M, Xu X G and Rivard M J 2010 Comparison of organ doses for patients undergoing balloon brachytherapy of the breast with HDR ^{192}Ir or electronic sources using Monte Carlo simulations in a heterogeneous human phantoma *Med. Phys.* **37** 662–71

Nunn A A, Davis S D, Micka J A and DeWerd L A 2008 LiF:Mg,Ti TLD response as a function of photon energy for moderately filtered x-ray spectra in the range of 20–250 kVp relative to ^{60}Co *Med. Phys.* **35** 1859–69

Perkins S T *et al* 1997 Table and graphs of atomic subshell and relaxation data derived from the LLNL evaluated atomic data library (EADL) UCRL-50400 **30**

Rivard M J, Davis S D, DeWerd L A, Rusch T W and Axelrod S 2006 Calculated and measured brachytherapy dosimetry parameters in water for the Xoft Axxent x-ray source: an electronic brachytherapy source *Med. Phys.* **33** 4020–32

Sutherland J G H and Rogers D W O 2010 Monte Carlo calculated absorbed-dose energy dependence of EBT and EBT2 film *Med. Phys.* **37** 1110–6

van Hoof S, Granton P, Landry G, Podesta M and Verhaegen F 2012 Evaluation of a novel triple-channel radiochromic film analysis procedure using EBT2 *Phys. Med. Biol.* **57** 4353–68

White S A *et al* 2014 Comparison of TG-43 and TG-186 in breast irradiation using a low energy electronic brachytherapy source *Med. Phys.* **41** 061701